

ELECTRONIC SUPPLEMENTARY INFORMATION (ESI)

Formation in aqueous solution of non-oxido V^{IV} complex with VN₆ coordination. Potentiometric, ESI-MS, spectroscopic and computational characterization

Elzbieta Lodyga-Chruscinska,^a Agnieszka Szebesczyk,^b Daniele Sanna,^c Kaspar Hegetschweiler,^d Giovanni Micera^e and Eugenio Garribba^{e,*}

^a Institute of General Food Chemistry, Technical University of Lodz, ul. Stefanowskiego 4/10, PL-90924, Lodz, Poland

^b Faculty of Chemistry, University of Wrocław, 14 F. Joliot-Curie St., PL-50383, Wrocław, Poland

^c Istituto CNR di Chimica Biomolecolare, Trav. La Crucca 3, I-07040 Sassari, Italy

^d Fachrichtung Chemie, Universität des Saarlandes, Postfach 15 11 50, D-66041 Saarbrücken, Germany

^e Dipartimento di Chimica e Farmacia, and Centro Interdisciplinare per lo Sviluppo della Ricerca Biotecnologica e per lo Studio della Biodiversità della Sardegna, Università di Sassari, Via Vienna 2, I-07100 Sassari, Italy. E-mail: garribba@uniss.it; Fax: +39 079 229559; Tel: +39 079 229487.

EPR theory background

The ^{51}V HFC tensor A has three contributions: the isotropic Fermi contact (A^{FC}), the anisotropic or dipolar hyperfine interaction (A^{D}), and the second-order term that arises from spin-orbit (SO) coupling (A^{SO}):¹

$$A = A^{\text{FC}} \mathbf{1} + A^{\text{D}} + A^{\text{SO}} \quad (1)$$

where $\mathbf{1}$ is the unit tensor; A^{FC} and the components $A_{\mu\nu}^{\text{D}}$ and $A_{\mu\nu}^{\text{SO}}$ of the tensors A^{D} and A^{SO} are given by the following equations:

$$A^{\text{FC}} = \frac{4\pi}{3} g_e g_N \beta_e \beta_N \langle S_z \rangle^{-1} \rho_N^{\alpha-\beta} \quad (2)$$

$$A_{\mu\nu}^{\text{D}} = \frac{1}{2} g_e g_N \beta_e \beta_N \langle S_z \rangle^{-1} \sum_{k,l} P_{k,l}^{\alpha-\beta} \langle \Phi_k | \frac{\mathbf{r}^2 \delta_{\mu\nu} - 3\mathbf{r}_\mu \mathbf{r}_\nu}{\mathbf{r}^5} | \Phi_l \rangle \quad (3)$$

$$A_{\mu\nu}^{\text{SO}} = -\frac{1}{2S} g_e g_N \beta_e \beta_N \sum_{k,l} \frac{\partial P_{k,l}^{\alpha-\beta}}{\partial I_\mu} \langle \Phi_k | h_\nu^{\text{SOC}} | \Phi_l \rangle \quad (4)$$

g_e and g_N are the g -factors of the free electron and the nucleus, β_e and β_N the electron and nuclear magnetons, $\langle S_z \rangle$ the expectation value of the electronic spin on the z axis, $\rho_N^{\alpha-\beta}$ the spin density at the nucleus, $P_{k,l}^{\alpha-\beta}$ the spin density matrix, \mathbf{r} the distance between the unpaired electron and the nucleus, and h_ν^{SOC} the spatial part of an effective one-electron spin-orbit operator.¹

The tensor A^{D} is always traceless: A_x^{D} , A_y^{D} and A_z^{D} are the elements of the diagonalized tensor, their sum being zero:

$$A_x^{\text{D}} + A_y^{\text{D}} + A_z^{\text{D}} = 0 \quad (5)$$

The values of the ^{51}V anisotropic hyperfine coupling constants along the x , y and z axes result to be:

$$A_x = A^{\text{FC}} + A_x^{\text{D}} + A_x^{\text{SO}} \quad (6)$$

$$A_y = A^{\text{FC}} + A_y^{\text{D}} + A_y^{\text{SO}} \quad (7)$$

$$A_z = A^{\text{FC}} + A_z^{\text{D}} + A_z^{\text{SO}} \quad (8)$$

From eqs. (5)-(8), the value of A_{iso} is:

$$A_{\text{iso}} = \frac{1}{3}(A_x + A_y + A_z) = A^{\text{FC}} + \frac{1}{3}(A_x^{\text{SO}} + A_y^{\text{SO}} + A_z^{\text{SO}}) = A^{\text{FC}} + A^{\text{PC}} \quad (9)$$

The term $\frac{1}{3}(A_x^{\text{SO}} + A_y^{\text{SO}} + A_z^{\text{SO}})$ is named isotropic pseudocontact, A^{PC} .¹

Gaussian neglects the second-order SO effects and eqs. (6)-(9) become:

$$A_x = A^{\text{FC}} + A_x^{\text{D}} \quad (10)$$

$$A_y = A^{\text{FC}} + A_y^{\text{D}} \quad (11)$$

$$A_z = A^{\text{FC}} + A_z^{\text{D}} \quad (12)$$

$$A_{\text{iso}} = A^{\text{FC}} \quad (13)$$

Table S1 Main calculated and experimental electronic transitions calculated for $[\text{VO}(\text{taci})(\text{H}_2\text{O})_2]^{2+}$, $[\text{VO}(\text{tmca})(\text{H}_2\text{O})_2]^{2+}$, $[\text{V}(\text{taci})_2]^{4+}$ and $[\text{V}(\text{tmcaH}_{-2})_2]$ till 300 nm.

	Main transition	Character (%)	λ^a	$f \times 10^5 b$	$\lambda^{\text{exptl}} / \varepsilon^{\text{exptl}} a,c$
$[\text{VO}(\text{taci})(\text{H}_2\text{O})_2]^{2+}$	$\text{H}(\alpha) \rightarrow \text{L}(\alpha)$	$d_{xy} \rightarrow d_{xz}$ (66.3)	781.4	20	845 / 15
	$\text{H}(\alpha) \rightarrow \text{L}+1(\alpha)$	$d_{xy} \rightarrow d_{yz}$ (79.6)	645.3	10	608 / 5
	$\text{H}(\alpha) \rightarrow \text{L}+3(\alpha)$	$d_{xy} \rightarrow d_{x^2-y^2}$ (61.8)	464.6	10	560 / 10
	$\text{H}(\alpha) \rightarrow \text{L}+6(\alpha)$	$d_{xy} \rightarrow d_z^2$ (53.6)	335.6	30	370 / 190
$[\text{VO}(\text{tmca})(\text{H}_2\text{O})_2]^{2+ d}$	$\text{H}-1(\alpha) \rightarrow \text{L}(\alpha)$	$d_{xy} \rightarrow d_{xz}$ (75.9)	645.6	30	680 / 20
	$\text{H}-1(\alpha) \rightarrow \text{L}+1(\alpha)$	$d_{xy} \rightarrow d_{yz}$ (77.2)	586.0	10	
	$\text{H}-1(\alpha) \rightarrow \text{L}+2(\alpha)$	$d_{xy} \rightarrow d_{x^2-y^2}$ (82.4)	502.8	10	
$[\text{V}(\text{taci})_2]^{4+}$	$\text{H}(\alpha) \rightarrow \text{L}(\alpha)$	$d_{xy} \rightarrow d_{yz}$ (87.2)	2046.1	5	
	$\text{H}(\alpha) \rightarrow \text{L}+1(\alpha)$	$d_{xy} \rightarrow d_{xz}$ (87.3)	1965.3	5	
	$\text{H}-3(\alpha) \rightarrow \text{L}(\alpha) / \text{O}^{\text{lp}} \rightarrow d_{yz}$ (35.1)		413.1	110	
	$\text{H}-1(\alpha) \rightarrow \text{L}+1(\alpha)$	$\text{O}^{\text{lp}} \rightarrow d_{xz}$ (29.1)			
	$\text{H}-2(\alpha) \rightarrow \text{L}+1(\alpha)$	$\text{O}^{\text{lp}} \rightarrow d_{xz}$ (62.8)	403.7	2250	375 / 1190
	$\text{H}-1(\beta) \rightarrow \text{L}(\beta)$	$\text{O}^{\text{lp}} \rightarrow d_{xy}$ (49.3)	337.5	470	
	$\text{H}-1(\beta) \rightarrow \text{L}(\beta)$	$\text{O}^{\text{lp}} \rightarrow d_{xy}$ (36.8)	333.5	500	
	$\text{H}-8(\alpha) \rightarrow \text{L}(\alpha)$	$\text{O}^{\text{lp}} \rightarrow d_{yz}$ (35.4)	316.0	4890	295 / 1790
$[\text{V}(\text{tmcaH}_{-2})_2]$	$\text{H}(\alpha) \rightarrow \text{L}(\alpha)$	$d_{xy} \rightarrow d_{yz}$ (95.0)	1091.3	5	
	$\text{H}(\alpha) \rightarrow \text{L}+1(\alpha)$	$d_{xy} \rightarrow d_{xz}$ (90.2)	898.1	10	
	$\text{H}-1(\alpha) \rightarrow \text{L}(\alpha)$	$\text{N}^{\text{lp}} \rightarrow d_{yz}$ (52.6)	548.0	800	
	$\text{H}-2(\alpha) \rightarrow \text{L}(\alpha)$	$\text{N}^{\text{lp}} \rightarrow d_{yz}$ (70.8)	530.6	2770	480 / 935
	$\text{H}-1(\alpha) \rightarrow \text{L}+1(\alpha)$	$\text{N}^{\text{lp}} \rightarrow d_{xz}$ (60.7)	478.8	370	
	$\text{H}(\beta) \rightarrow \text{L}(\beta)$	$\text{N}^{\text{lp}} \rightarrow d_{yz}$ (60.3)	376.0	830	395 / 1335 ^e
	$\text{H}(\beta) \rightarrow \text{L}+2(\beta)$	$\text{N}^{\text{lp}} \rightarrow d_{xz}$ (72.8)	361.6	740	
	$\text{H}-1(\beta) \rightarrow \text{L}+1(\beta)$	$\text{N}^{\text{lp}} \rightarrow d_{xy}$ (55.1)	356.2	760	
	$\text{H}-1(\beta) \rightarrow \text{L}+2(\beta)$	$\text{N}^{\text{lp}} \rightarrow d_{xz}$ (42.0)	335.6	6920	
	$\text{H}(\beta) \rightarrow \text{L}+2(\beta)$	$\text{N}^{\text{lp}} \rightarrow d_{xz}$ (32.7)	333.2	20250	320 / 7100

^a λ values measured in nm. ^b Oscillator strength. ^c ε values measured in $\text{M}^{-1} \text{cm}^{-1}$. ^d $d_{xy} \rightarrow d_z^2$ predicted at 281.1 nm. ^e Shoulder of a more intense absorption.

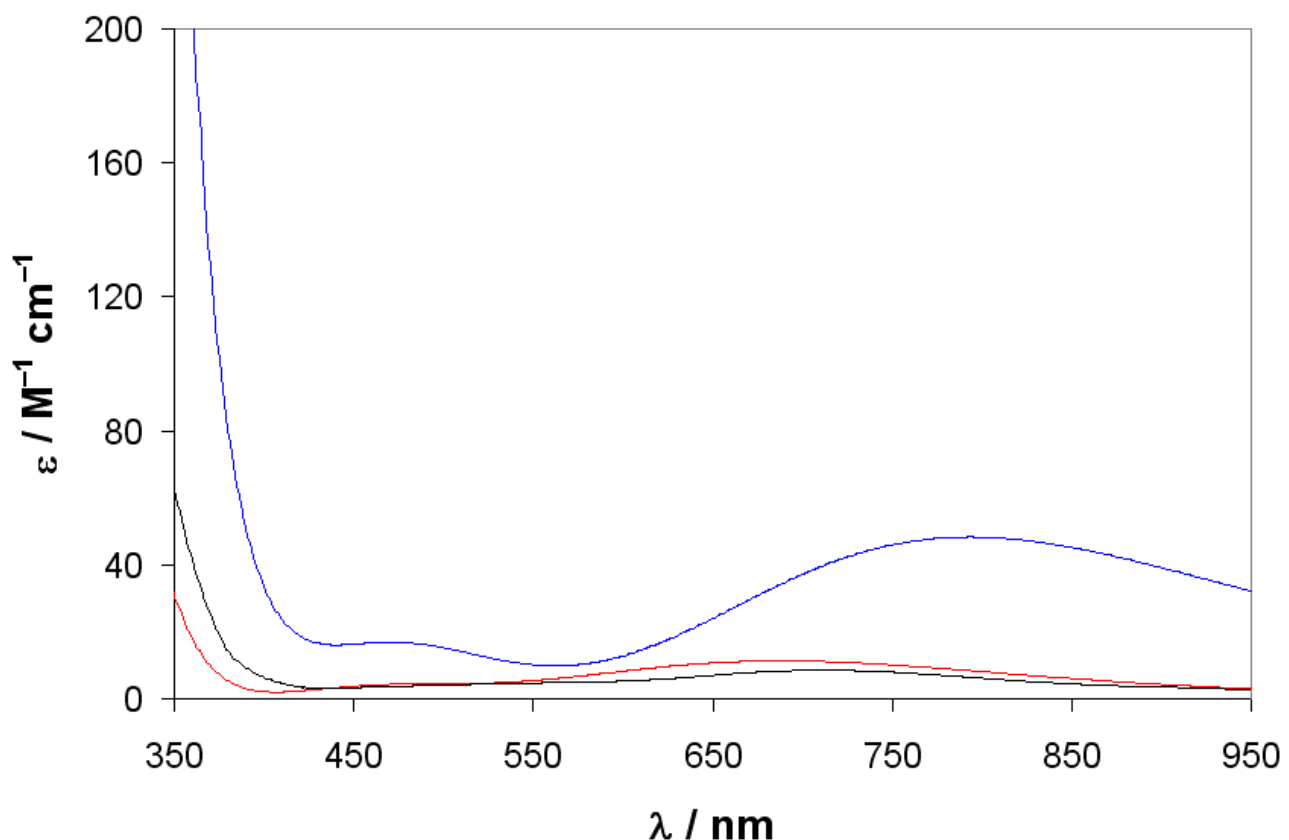


Fig. S1 Experimental electronic absorption spectrum of $[\text{VOLH}_{-1}]^+$, recorded on the $\text{V}^{\text{IV}}\text{O}^{2+}/\text{tmca}$ (L) system with a total $\text{V}^{\text{IV}}\text{O}^{2+}$ concentration of 4×10^{-3} M, $L/\text{V}^{\text{IV}}\text{O} = 15$, pH 7.05 (in black). The spectra calculated by DFT methods for the two possible species $[\text{VO(tmca)(OH)(H}_2\text{O)}]^+$ and $[\text{VO(tmcaH-1)(H}_2\text{O)}_2]^+$ are shown in red and blue, respectively.

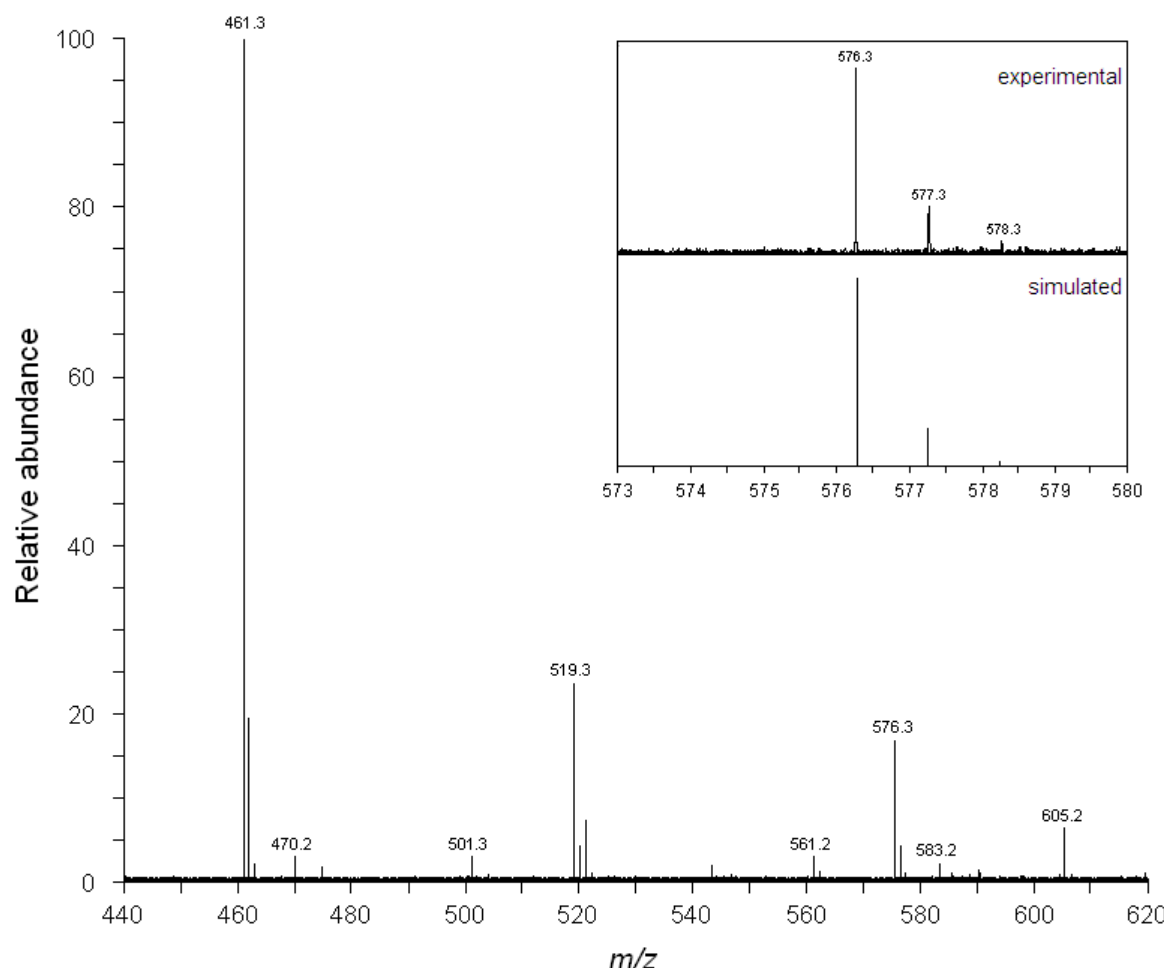


Fig. S2 ESI positive ion mass spectrum recorded on the $\text{V}^{\text{IV}}\text{O}^{2+}/\text{tmca}$ (L) system in a mixture $\text{MeOH}/\text{H}_2\text{O}$ 1:1 v/v with a total L concentration of 1.0×10^{-4} M, $\text{L}/\text{V}^{\text{IV}}\text{O} = 15$, pH 10.30. In the inset the region between m/z 573 and 580. The peaks at m/z 461.3 and 519.3 were assigned to the ions $\{2\text{tmca} + \text{Na}^+\}$ and $\{2\text{tmca} + \text{NaCl} + \text{Na}^+\}$, that at m/z of 576.3 to $\{[\text{V}(\text{tmcaH}_{-2})_2] + \text{Na}^+ + 2\text{H}_2\text{O} + \text{MeOH}\}$.

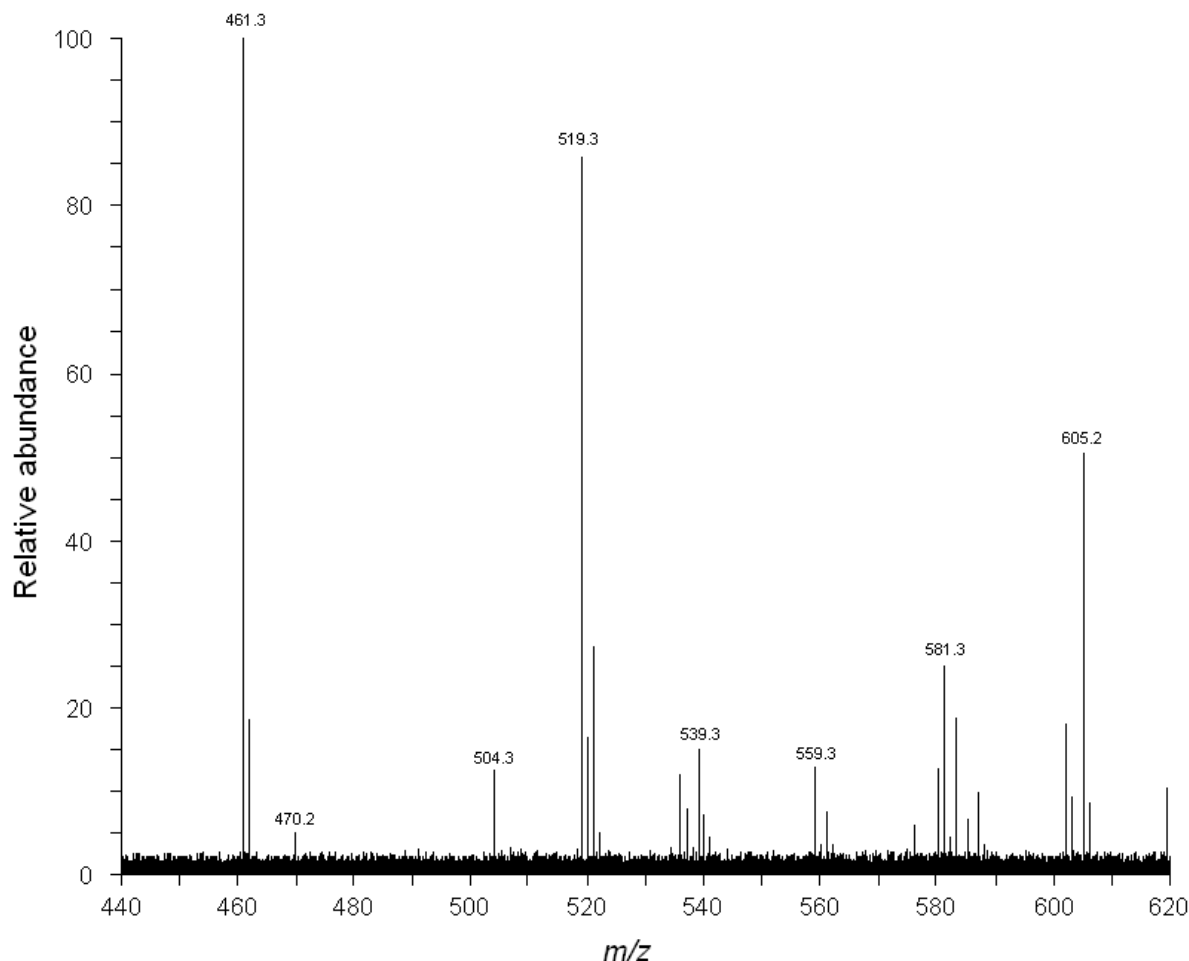


Fig. S3 ESI positive ion mass spectrum recorded on the $\text{V}^{\text{IV}}\text{O}^{2+}/\text{tmca}$ (L) system in a mixture MeOH/H₂O 1:1 v/v with a total L concentration of 1.0×10^{-4} M, L/ $\text{V}^{\text{IV}}\text{O}$ = 15, pH 5.20. The peaks at m/z 461.3 and 519.3 were assigned to the ions $\{\text{2tmca} + \text{Na}^+\}$ and $\{\text{2tmca} + \text{NaCl} + \text{Na}^+\}$.

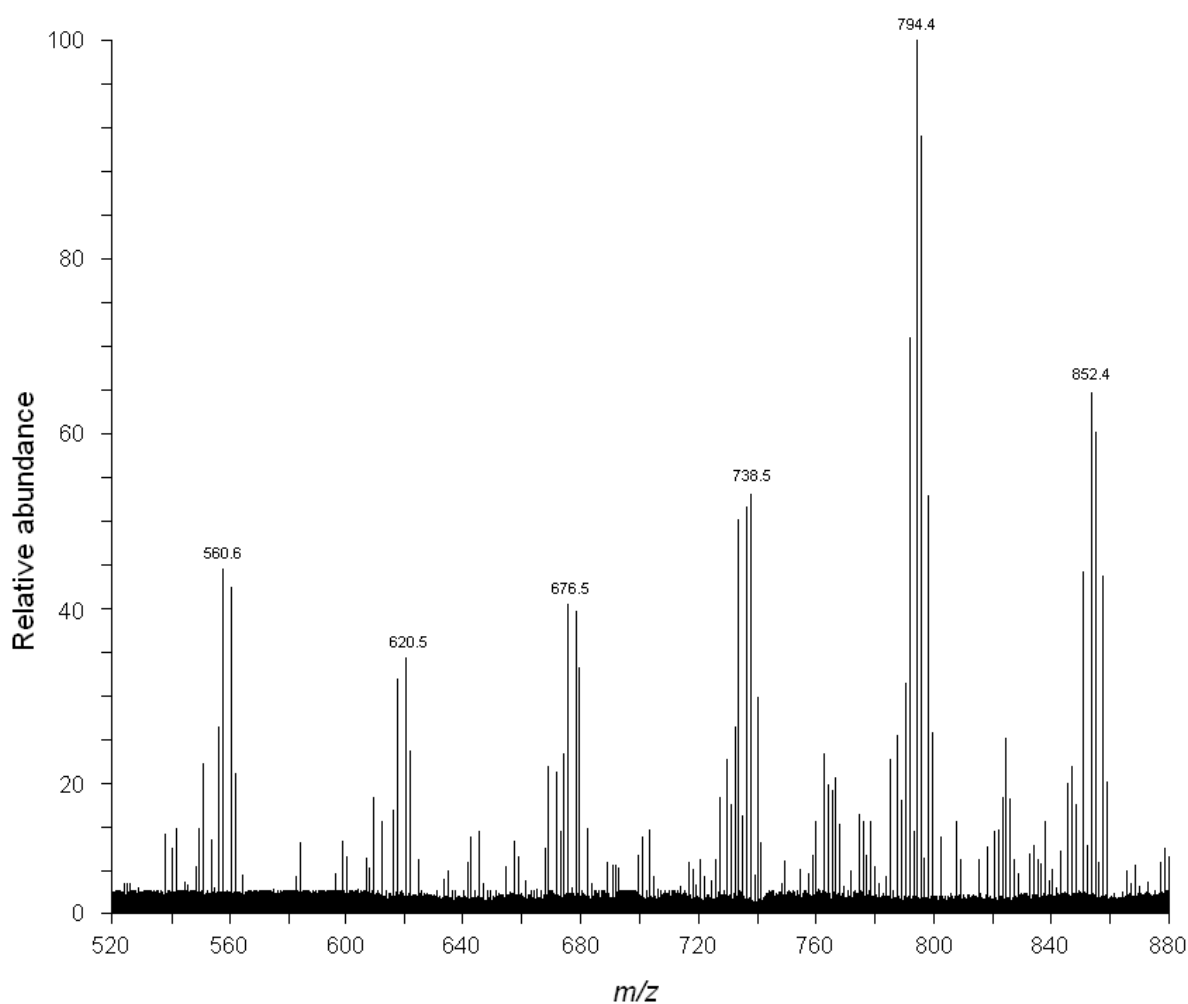


Fig. S4 ESI negative ion mass spectrum recorded on the $\text{V}^{\text{IV}}\text{O}^{2+}$ /tmca (L) system in a mixture MeOH/H₂O 1:1 v/v with a total L concentration of 1.0×10^{-4} M, $\text{L}/\text{V}^{\text{IV}}\text{O} = 15$, pH 10.30. The peaks at m/z 560.6 and 676.5 were assigned to the ions $\{[\text{V(tmcaH}_2\text{)}_2] + \text{NaCl} + \text{OH}^-\}$ and $\{[\text{V(tmcaH}_2\text{)}_2] + \text{NaCl} + 2\text{H}_2\text{O} + \text{SO}_4^{2-}\}$, those at m/z 794.4 and 852.4 to $\{[\text{VO(OH)}_3]^+ + 5\text{NaCl} + \text{Cl}^- + \text{OH}^- + \text{SO}_4^{2-}\}$ and $\{[\text{VO(OH)}_3]^+ + 6\text{NaCl} + \text{Cl}^- + \text{OH}^- + \text{SO}_4^{2-}\}$.

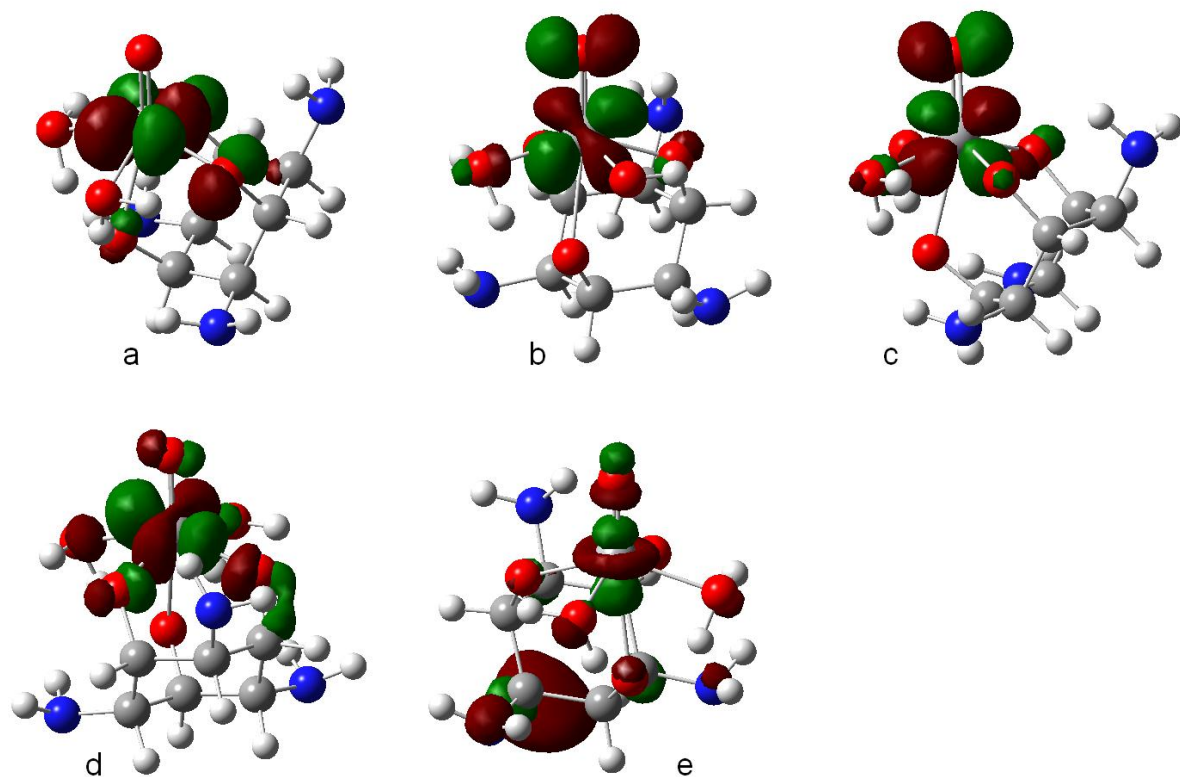


Fig. S5 Molecular orbitals for $[\text{VO}(\text{taci})(\text{H}_2\text{O})_2]^{2+}$: (a) $\text{H}(\alpha)$, $\text{V}-d_{xy}$, (b) $\text{L}(\alpha)$, $\text{V}-d_{xz}$, (c) $\text{L}+1(\alpha)$, $\text{V}-d_{yz}$, (d) $\text{L}+3(\alpha)$, $\text{V}-d_{x^2-y^2}$ and (e) $\text{L}+6(\alpha)$, $\text{V}-d_z^2$.

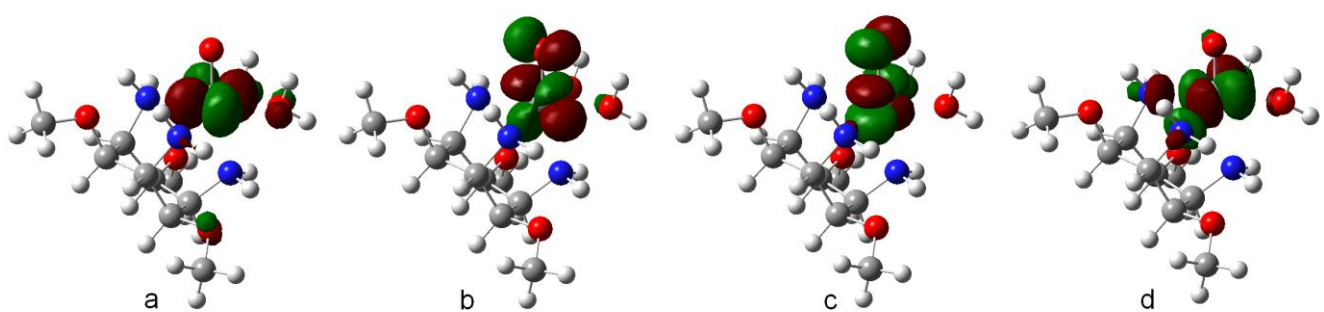


Fig. S6 Molecular orbitals for $[\text{VO}(\text{tmca})(\text{H}_2\text{O})_2]^{2+}$: (a) $\text{H}-1(\alpha)$, $\text{V}-d_{xy}$, (b) $\text{L}(\alpha)$, $\text{V}-d_{xz}$, (c) $\text{L}+1(\alpha)$, $\text{V}-d_{yz}$ and (d) $\text{L}+2(\alpha)$, $\text{V}-d_{x^2-y^2}$.

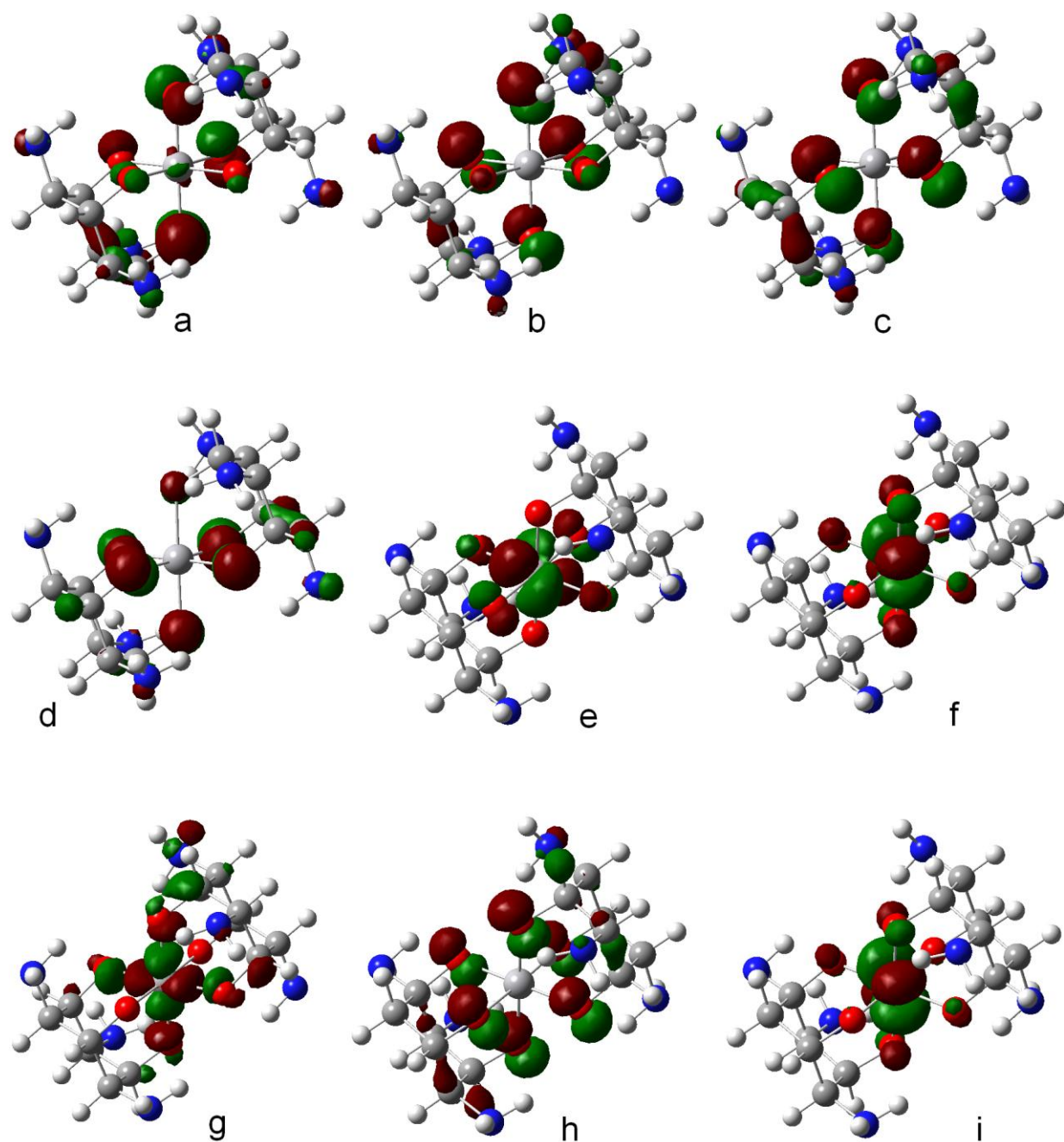


Fig. S7 Molecular orbitals for $[V(\text{taci})_2]^{4+}$: (a) H-8(α), tacn-O^{lp}, (b) H-3(α), tacn-O^{lp}, (c) H-2(α), tacn-O^{lp}, (d) H-1(α), tacn-O^{lp}, (e) H(α), V-d_{xy}, (f) L(α), V-d_{yz}, (g) L+1(α), V-d_{xz}, (h) H-1(β), tacn-O^{lp} and (i) L(β), V-d_{xy}. The superscript lp indicates an electron lone pair.

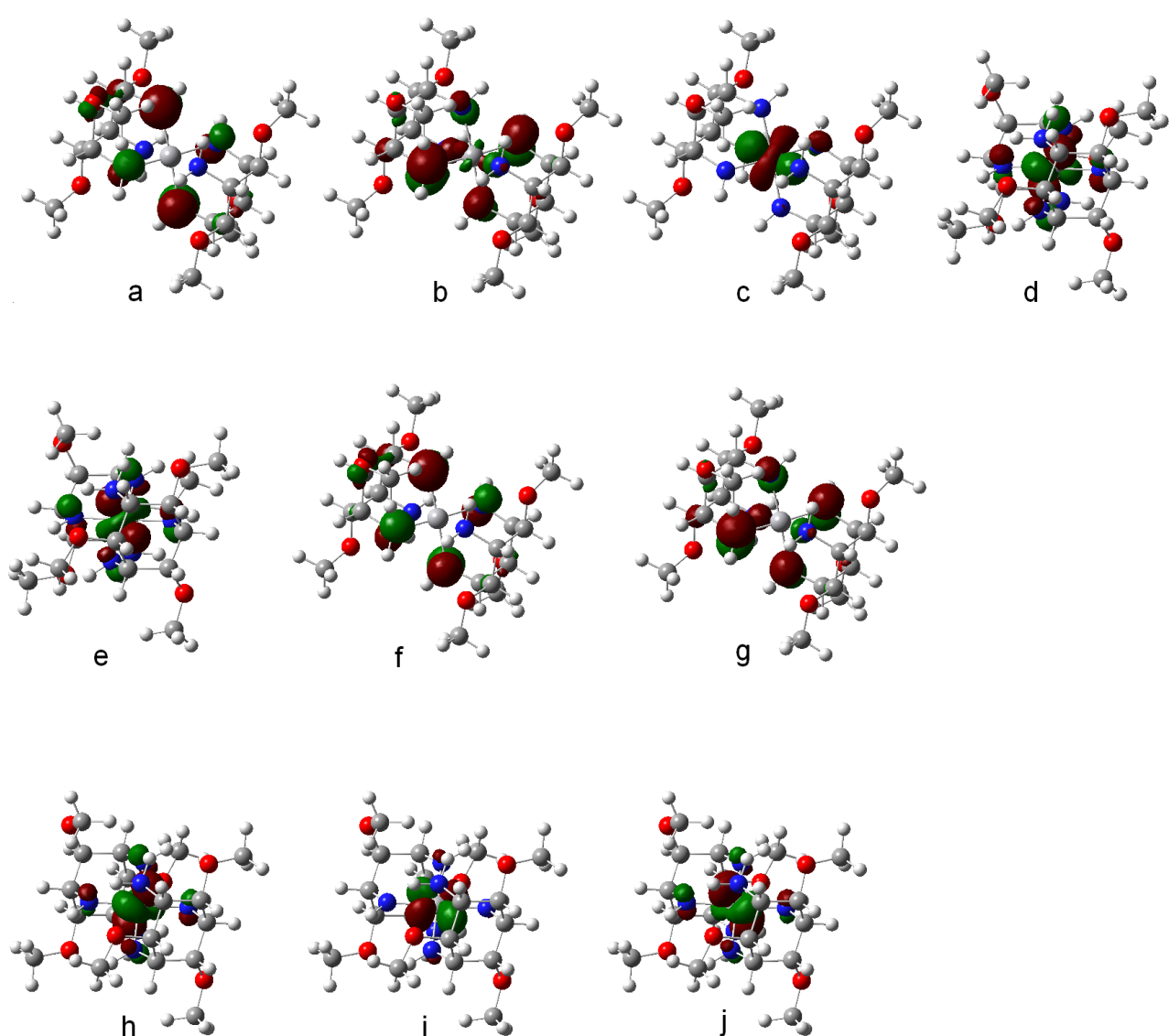


Fig. S8 Molecular orbitals for $[V(\text{tmcaH}_2)_2]$: (a) H-2(α), tmca-N^{lp}, (b) H-1(α), tmca-N^{lp}, (c) H(α), V-d_{xy}, (d) L(α), V-d_{yz}, (e) L+1(α), V-d_{xz}, (f) H-1(β), tmca-N^{lp}, (g) H(β), tmca-N^{lp}, (h) L(β), V-d_{yz}, (h) L+1(β), V-d_{xy}, and (i) (h) L+2(β), V-d_{xz}. The superscript lp indicates an electron lone pair.

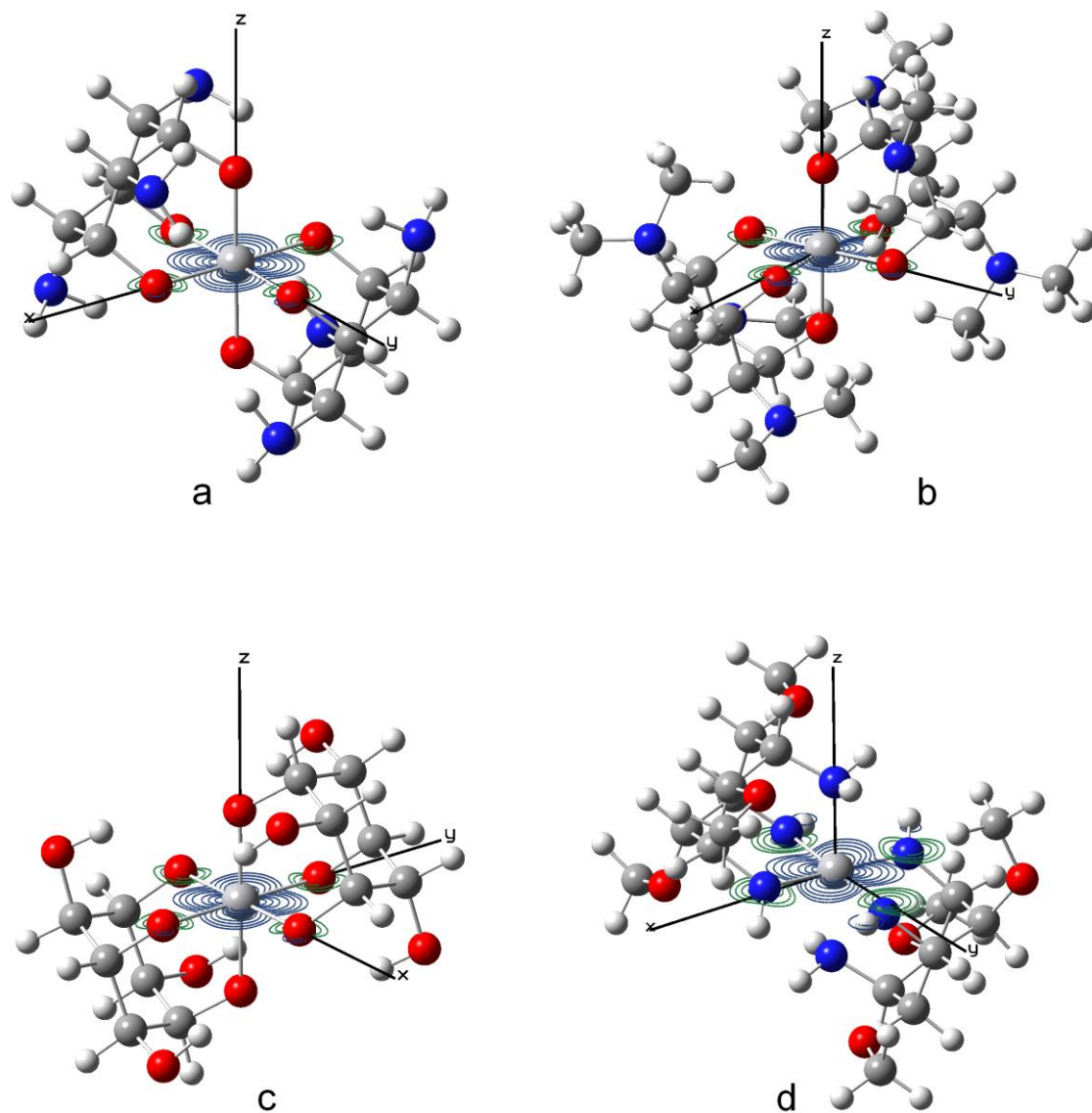
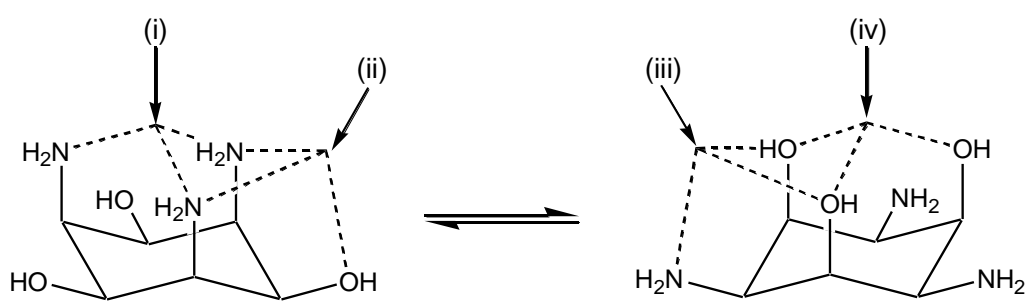
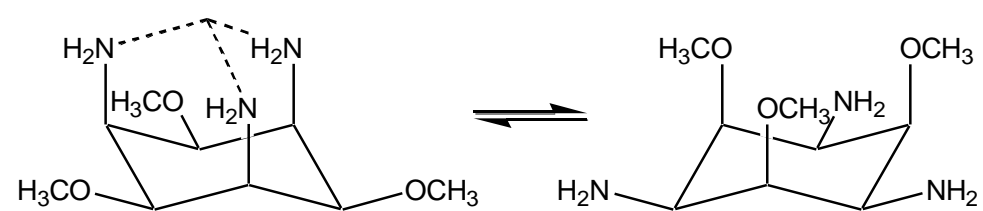


Fig. S9 Spin density contour of (a) $[\text{V}(\text{taci})_2]^{4+}$, (b) $[\text{V}(\text{tdci})_2]^{4+}$, (c) $[\text{V}(\text{inoH}_3)_2]^{2-}$ and (d) $[\text{V}(\text{tmcaH}_2)_2]$. The three Cartesian axes are also represented.



Scheme S1 Possible coordination modes of a papa ligand.



Scheme S2 The two chair conformations of tmca.

References

1. F. Neese, *ORCA - An Ab Initio, DFT and Semiempirical Program Package, Version 2.9*, Max-Planck-Institute for Bioinorganic Chemistry, Mülheim a. d. Ruhr, Germany, 2012.